International Journal of Nanomedicine

Dovepress

open access to scientific and medical research

Open Access Full Text Article

ORIGINAL RESEARCH

Effects of Simvastatin-Loaded Nanomicelles on the Early Preservation of Tooth Extraction Sites

Xianling Feng[1,*], Fucheng Tao[2,*], Min Ren[3,*], Mao Niu[4]

[1]School of Medical, Shenzhen University, Shenzhen, 518060, People's Republic of China; [2]Department of Stomatology, Shenzhen University General Hospital, Shenzhen, 518055, People's Republic of China; [3]Department of Stomatology, Rizhao Traditional Chinese Medicine Hospital, Rizhao, 276800, People's Republic of China; [4]School of Medical Technology and Nursing, Shenzhen Polytechnic University, Shenzhen, 518055, People's Republic of China

*These authors contributed equally to this work

Correspondence: Mao Niu, School of Medical Technology and Nursing, Shenzhen Polytechnic University, 7098 Liuxian Avenue, Nanshan District, Shenzhen, 518055, People's Republic of China, Tel +86 755 26011160, Fax +86 755 26018477, Email niu1037@szpu.edu.cn

Object: The present study intended to evaluate the effect of simvastatin-loaded nanomicelles (SVNs) on promoting new bone formation and reducing alveolar ridge resorption at the tooth extraction sites at the early healing of the extraction sockets.

Methods: SVNs were synthesized using a dialysis method. The rabbit tooth extraction model was established, SVNs and simvastatin (SV) were loaded on gelatin sponge and inserted into the extraction socket. CBCT scans were performed at 0, 2, and 4 weeks postoperatively to evaluate bone formation and alveolar ridge absorption in the extraction sockets. And all the animals were sacrificed and the mandibles were harvested. And HE staining and Masson staining were used for histological evaluation of the bone formation in the extraction sockets.

Results: Radiographic evaluation showed that compared with the blank control group, at 2 and 4 weeks after extraction, SVNs increased the new bone density in the extraction sockets by 75.7% and 96.5%, and reduced the absorption rate of alveolar ridge length at the extraction sites by 60.8% and 49.1%, respectively. Histological evaluation showed that SVNs significantly improved the maturation of new bone tissue in the extraction sockets.

Conclusion: SVNs can significantly accelerate healing and effectively reduce the absorption of alveolar ridge at the extraction sites in the early stage of tooth extraction socket healing.

Keywords: alveolar ridge preservation, simvastatin-loaded nanomicelles, tooth extraction sites, bone formation

Introduction

After tooth extraction, alveolar bone atrophy in the extraction socket area, especially resorption of the alveolar ridge, inevitably occurs.[1] Alveolar bone resorption can occur as soon as the first three months after tooth extraction. The resorption amount can reach 40–60% in the first 2 to 3 years after tooth extraction and continues at a resorption rate of 0.25–0.5% per year afterwards.[2,3] Alveolar bone atrophy seriously affects subsequent oral restorative treatment. Especially in oral implant restoration, the difficulty in implant placement is caused by insufficient bone quantity in the implanted area. As a result, expensive bone grafting surgery is usually required, which not only increases the treatment trauma and cost for the patient but also greatly prolongs the time for implant restoration treatment.[4] Therefore, during tooth extraction, the preservation of the extraction site, otherwise known as alveolar ridge preservation (ARP), has become an important part of clinical oral treatment.

Commonly used ARP techniques include minimally invasive tooth extraction, immediate implantation, and bone or synthetic bone substitute grafting techniques. Bone or bone substitute grafting is currently the most commonly used ARP technique.[5] Bone grafts include autologous bone grafts and allogeneic bone grafts. Autologous bone grafting is the gold standard for repairing bone defects, but it has drawbacks such as limited available quantities and complications such as bleeding, pain, and infection. The main source of allogeneic bone is the calf bone, which is harvested and used in clinical practice. Although suitable therapeutic effects have been achieved, there are potential risks of virus transmission and

Received: 2 August 2024
Accepted: 14 September 2024
Published: 1 October 2024

© 2024 Feng et al. This work is published and licensed by Dove Medical Press Limited. The full terms of this license are available at https://www.dovepress.com/terms.php and incorporate the Creative Commons Attribution – Non Commercial (unported, v3.0) License (http://creativecommons.org/licenses/by-nc/3.0/). By accessing the work you hereby accept the Terms. Non-commercial uses of the work are permitted without any further permission from Dove Medical Press Limited, provided the work is properly attributed. For permission for commercial use of this work, please see paragraphs 4.2 and 5 of our Terms (https://www.dovepress.com/terms.php).

immune rejection.[6,7] The most commonly used synthetic bone substitute materials include dual-phase calcium phosphate ceramics, tricalcium phosphate cement, and bioactive ceramics[8–10] Synthetic bone substitutes overcome the shortcomings of the above two materials; however, some researchers believe that the use of these graft materials may interfere with the normal healing process in the extraction socket. To combat the potential negative effects of synthetic bone materials, exogenous osteogenic growth factors such as recombinant human bone morphogenetic protein-2 (rhBMP-2) have been added to bone substitute materials[11,] and scholars have confirmed that the addition of osteogenic growth factors can significantly improve the effect of these materials on ARP.[12,13] However, exogenous osteogenic growth factors are currently expensive and have a short half-life. Therefore, mobilizing endogenous osteogenic growth factors to improve the effect of ARP is a topic worthy of exploration.

Mundy et al studied more than 30,000 compounds and reported that statins, especially simvastatin (SV), significantly promoted new bone formation in the mouse calvarial region by increasing the expression of BMP-2 in osteoblasts in vivo.[14] Therefore, SV is expected to replace rhBMP-2 as a synthetic bone supplement to improve ARP, and the cost of SV is 16,000 times less than that of BMP-2.[14] Moreover, some researchers have recently mixed SV with collagen and implanted it in the extraction socket, and SV significantly promoted new bone formation in the extraction socket and effectively slowed the resorption of the alveolar ridge.[15] Hence, SV has broad application prospects for promoting jaw defect repair and the healing of extraction sockets (ie, ARP) by regulating endogenous osteogenic growth factors. However, because SV is a fat-soluble drug, it is insoluble in water and has low bioavailability.

The application of various nanodrug carriers to encapsulate and deliver SV can significantly improve their osteogenic effect both in vivo and in vitro. Some scholars[16] have used nanoliposome-encapsulated SV to treat bone marrow-derived mesenchymal stem cells (BMSCs) and found that compared with SV, SV-loaded nanoliposomes (SVNs) significantly improved ALP and increased BMP-2 expression in BMSCs, significantly promoting osteogenesis. Other researchers[17] synthesized SVNs to treat MG63 cells and similarly found that they had a stronger osteogenic effect than free SV. In in vivo studies, several researchers[18] have implanted SV-PLGA-loaded nanomicelles into the bone defect region at the top of the rabbit skull for osteogenesis experiments and found that the drug-loaded nanomicelles exhibited a sustained release effect for up to 1 month, and significantly promoted new bone formation in the bone defect area. Some scholars[19] implanted synthetic SV-PGLA-loaded nanomicelles into rat extraction sockets and significantly promoted new bone formation in the extraction sockets compared with that in the control group.

Our previous studies[20,21] showed that SVNs synthesized by using methoxy-PEG (mPEG-) PLA to encapsulate SVNs not only exhibited a stronger osteogenic effect than SV in vitro but also significantly upregulated the protein expression of osteogenesis-related factors such as ALP, OC, and OSX in osteoblasts. Moreover, SVNs have been mixed with bone powder or a gelatin sponge to repair rabbit calvarial defects. According to quantitative and qualitative radiological and histomorphometric analyses of new bone in the bone defect area, SVNs mixed with bone powder or gelatin were confirmed to have greater in vivo osteogenic efficacy than SV. In the present study, we mixed an SVNs solution with gelatin to form an SVNs gelatin-based sponge and placed them in a rabbit extraction socket to evaluate the ability of SVNs to promote new bone formation in the extraction socket and reduce alveolar ridge resorption at the tooth extraction sites in the early stage of tooth extraction socket healing. This study provided basic evidence for the successful application of the nano-dosage form of SV in ARP techniques.

Materials and Methods

Synthesis and Characterization of SVNs

Based on our previous experience in nanomicelle preparation, SVNs (mPEG-PLA-SV) were prepared using a dialysis method.[21] Then, 25 mg of mPEG-PLA (Jinan Daigang Biomaterial Co., Ltd., Shandong, China) and 5 mg of SV (National Institutes for Food and Drug Control, Beijing, China) were fully dissolved in 5 mL of acetone solution (Fisher Scientific, Waltham, MA, USA), added dropwise to 30 mL of deionized water, stirred for 60 min (500 rpm) at room temperature, ultrasonically dispersed, and transferred to a dialysis bag (MWCO3500) for 24 h to remove free drug, during which the water was changed every 1 h. The drug-free nanogels (DFNs) were also prepared in a similar way in the absence of SV.

The particle sizes of the SVNs and DFNs were measured using a Zetasizer instrument (Mastersizer 2000, Malvern Instruments Ltd., Malvern, UK). The nanomicelle morphology was observed with a transmission electron microscope (TEM; HT7700, Hitachi Limited, Tokyo, Japan). A high-performance liquid chromatography system (HPLC; LC-20AD, Shimadzu Corporation, Kyoto, Japan) was used to determine the drug loading capacity and encapsulation efficiency.

Experimental Animals

Ten healthy 5- to 6-month-old male New Zealand white rabbits weighing 2.17±0.17 kg were obtained from Shenzhen Advanced Medical Services Co., Ltd. Experimental procedures followed the Regulations for the Administration of Laboratory Animals of Guangdong Province and were approved by the Animal Ethics Committee at Shenzhen Polytechnic University. The rabbits were housed in a room with a standard room temperature of approximately 20 °C and a natural light cycle. They were fed standard rabbit feed (provided by Shenzhen Advanced Medical Service Co., Ltd.) with free access to drinking water every day. Feed consumption was recorded at regular intervals, and the rabbits were bred in individual cages. After 7 days of adaptive feeding, surgery was performed.

Surgical Procedure

All rabbits were fasted for 12 h before surgery and intramuscularly injected with 800,000 U of penicillin sodium 2 h before surgery. After injecting 0.3 mL/kg 3% pentobarbital sodium solution through the ear margin vein, the breathing of the animals was rapid and stable, with abdominal breathing mainly occurring. The corneal reflex was blunted and the systemic muscles were relaxed, indicating that the anaesthesia was successful. The bilateral mandibular central incisors were extracted from rabbits with minimal invasiveness, and the rabbits were randomly divided into 4 groups: no augmentation (blank control, BC), gelatin sponge (GS), gelatin sponge with 0.5 mg of SV (SV-GS), and gelatin sponge with 5 mg of SVNs (SVNs-GS). The four groups of experimental materials were randomly placed in four extraction sockets, and the sockets were tightly sutured.

Dental Cone Beam Computed Tomography (CBCT) Analysis

CBCT Scan

In vivo CBCT scans (3D MID, Planmeca, Finland) were performed on the experimental animals on the day of tooth extraction, 2 weeks after tooth extraction, and 4 weeks after tooth extraction (Figure 1). The scan parameters were a voltage of 70 kV, current of 9 mA, layer thickness of 0.2 mm, and exposure time of 12.351 s. CBCT software (Planmeca Romexis Viewer, Planmeca, Finland) was used for three-dimensional reconstruction of the scan data to observe and evaluate osteogenesis and ARP in the extraction socket.

Observation of New Bone Formation in the Extraction Socket

The qualitative evaluation of new bone formation in each experimental group was performed by observing 2D and 3D lateral radiographs of the extraction socket.

Quantitative Evaluation of New Bone Density in the Extraction Socket

Using BeeDicomViewer software (SinoUnion Healthcare Inc., Beijing, China), the alveolar socket area on each coronal image was selected as the region of interest (ROI), and the ROI in axial and sagittal images were automatically selected by the software (Figure 2A, green areas). All ROIs constituted the volume of interest (VOI), which was the entire alveolar socket. The software automatically calculated the mean CT value of the new bone in the alveolar socket, and the CT value was recorded as the mean bone density of the new bone in the extraction socket, in Hounsfield units (HU).

Comparison of 3D Images of Alveolar Ridge Morphology at the Extraction Site

The 3D reconstructed rabbit mandible image was exported as a 3D model in.STL format. Using Geomagic Qualify 12 software (Geomagic, Oqton Inc. USA), 3D models of the extraction socket area at 2 weeks and 4 weeks after tooth extraction were overlaid and aligned with the 3D model of the extraction socket area on the day of tooth extraction, after which 3D difference analysis was performed.

Figure 1 The experimental animals were scanned with CBCT.

Quantitative Evaluation of ARP in the Extraction Socket

The relative length of the alveolar ridge of the extraction socket in the 2D lateral radiographs was measured to evaluate the degree of ARP in each experimental group. The absolute length of the alveolar ridge of the extraction site was the distance from the anterior point of the lower central incisor to the highest point of the mesial alveolar ridge of the lower first premolar (Figure 2B, red line). The relative length of the alveolar ridge was calculated as follows: relative length of the alveolar ridge of the extraction socket = absolute length of the alveolar ridge 2–4 weeks after tooth extraction / absolute length of the alveolar ridge on the day of tooth extraction. The formula for calculating the resorption rate of the alveolar ridge length is as follows: 1 - relative length of the alveolar ridge in the extraction socket.

Histomorphometric Analysis

Four weeks after surgery, the animals were injected with 0.3 mL/kg 3% pentobarbital sodium solution through the ear margin for general anaesthesia. Then, the heart was perfused with 0.9% normal saline until the effluent became clear. The whole body of the animal was fixed in 10% neutral formalin through the heart for 30 min; after the rabbit became rigid, the mandible was harvested under sterile conditions and immediately soaked in 10% neutral formalin at room temperature for further fixation for 48 h. Then, each sample was soaked in decalcification solution (20% hydrochloric acid + 50% neutral formalin + 30% sodium chloride solution). After complete decalcification, the tooth extraction sockets were embedded in paraffin to prepare decalcified paraffin-embedded sections of new bone tissue at a thickness of 3–5 μm. The distribution of osteoblasts, the formation of new bone, the formation of neovasculature, and the trabecular bone structure in the extraction socket were observed using HE staining and Masson's trichrome staining, and qualitative analysis of the new bone tissue was performed at the two-dimensional level.

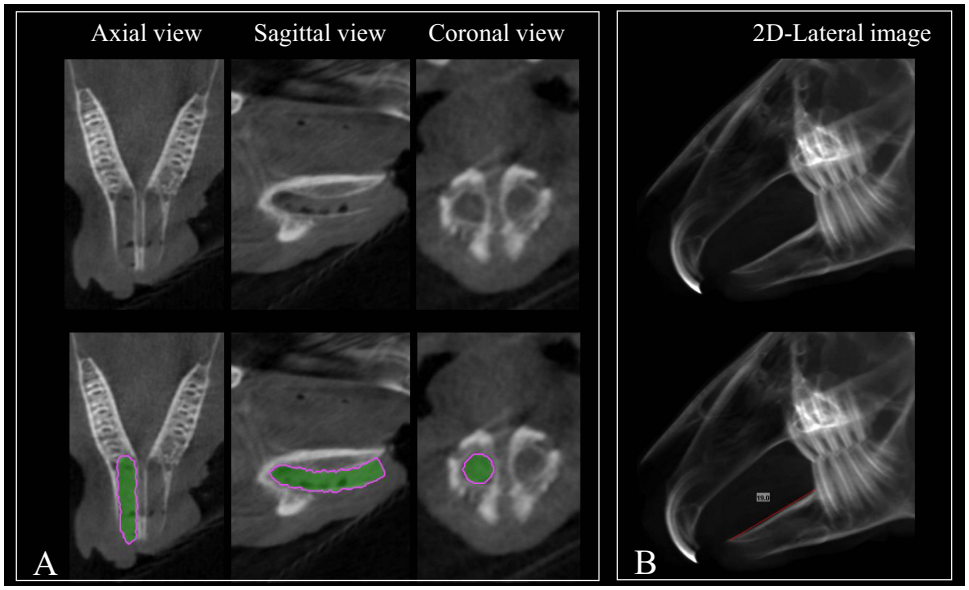

Figure 2 The new bone formation in the extraction socket and alveolar ridge absorption at the tooth extraction sites were analyzed by CBCT. (**A**) The green area was the region of interest (ROI) selected on each coronal, sagittal, and axial image of the extraction socket, respectively. (**B**) The distance between the anterior point of the lower central incisor and the highest point of the mesial alveolar ridge of the lower first premolar was measured as the absolute length of the alveolar ridge at the extraction sites and indicated by the red line.

Statistical Analysis

Statistical analysis was performed using SPSS Version 19.0 (IBM Corp., Armonk, NY, USA). All of the data are shown as the mean ± standard deviation (SD) from five independent experiments. The new bone density and the relative length of the alveolar ridge in the extraction socket were analysed by one-way repeated-measures ANOVA. A p value of <0.05 was deemed statistically significant.

Results

Characterization of SVNs

SVNs synthesized by dialysis had an encapsulation efficiency of 54.57±3.15%, a drug loading capacity of 10.91±0.63%, a particle size of 38.97±1.96 nm (Figure 3A). Transmission electron microscopy revealed that the drug-loaded nanomicelles were spherical in shape and uniform in size (Figure 3B).

Experimental Animals

The experimental animals healed well after the surgery, and there were no complications, such as swelling, infection, dehiscence or exposure of the surgical area. The number of samples in each group was 5, and the total number of samples was 20.

CBCT Analysis results

The 2D and 3D CT lateral radiographs of the extraction socket showed that on the day of tooth extraction, empty alveolar sockets could be seen in all the experimental groups, indicating that the teeth were completely extracted. Over time, the alveolar ridge tops at the extraction sites became rounded and blunt, and the length of the alveolar ridge became shorter to some extent in each experimental group, especially in the BC group. At 2 and 4 weeks after tooth extraction, new bone tissue formation was observed in all the experimental groups, with the SVNs-GS group having the highest density of new bone tissue. (Figure 4A)

The 3D models of the extraction site area were obtained through 3D reconstruction of the original CT data. Comparison of the 3D models of the alveolar ridge in the extraction socket at 2 and 4 weeks after tooth extraction and on the day of tooth extraction in each experimental revealed that as time after tooth extraction increased, there was some bone resorption of the alveolar ridge at the extraction site in each experimental group. In terms of alveolar ridge length, compared with that on

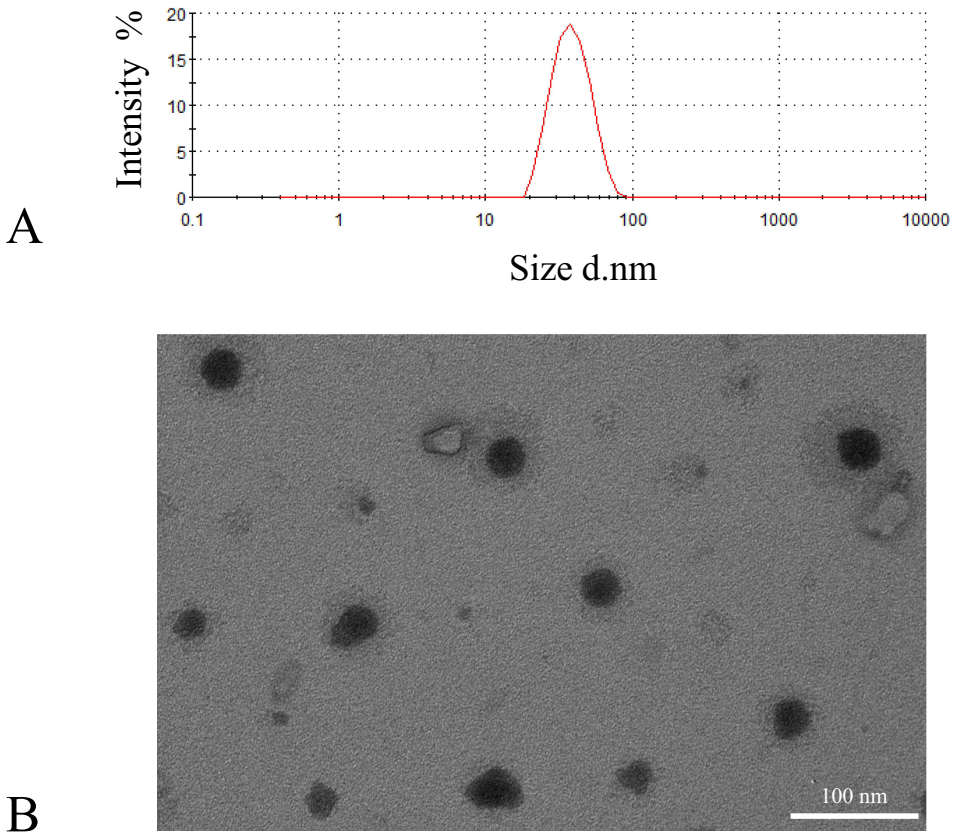

Figure 3 The characteristics of simvastatin-loaded nanomicelles. (**A**) The particle size of simvastatin-loaded nanomicelles were measured using a Zetasizer instrument. (**B**) The morphology of simvastatin-loaded nanomicelles morphology was observed with a transmission electron microscope (TEM).

the day of tooth extraction, there was significant bone resorption (gray area at the anterior end of the alveolar ridge) in the BC and GS groups, while the resorption in the SVNs-GS and SV-GS groups was relatively low. In addition, bone resorption also occurred on the surface of the alveolar ridge at the extraction site (blue area) in each experimental group. In particular, the blue area at 4 weeks was significantly larger than that at 2 weeks. At the same time point, the blue area on the bone surface was the smallest in the SVNs-GS group and the largest in the BC group. (Figure 4B)

Statistical analysis of the relative length of the alveolar ridge at the extraction site revealed that the extraction sites exhibited some degree of resorption over time. In each experimental group, the relative length of the alveolar ridge at the extraction site at 4 weeks was significantly shorter than that at 2 weeks. At the same time point, the relative length of the alveolar ridge at the extraction site in the SVNs-GS group and the SV-GS group was significantly longer than that in the BC group, while there was no significant difference between the GS group and the BC group. Among all the experimental groups, the relative length of the alveolar ridge in the SVNs-GS group was the longest. On this basis, the mean resorption rate of the alveolar ridge length at the extraction site in each experimental group at 2 weeks/4 weeks was as follows: 4.64%/7.51% in the SVNs-GS group, 7.00%/10.05% in the SV-GS group, 10.23%/13.76% in the GS group, and 11.85%/15.75% in the BC group. (Figure 4C)

In addition, the mean bone density of new bone in the extraction socket recorded in terms of CT values at 2 weeks/4 weeks was as follows: 730.58/1024.84 HU in the SVNs-GS group, 637.91/889.55 HU in the SV-GS group, 546.83/735.28 HU in the GS group, and 415.92/521.64 HU in the BC group. (Figure 4D)

Histological Analysis results

Under a 4× magnification, HE staining revealed the formation of woven bone in the new tissues of the extraction sockets in all the experimental groups. Among them, in the GS group, there remained blank areas that did not complete bone

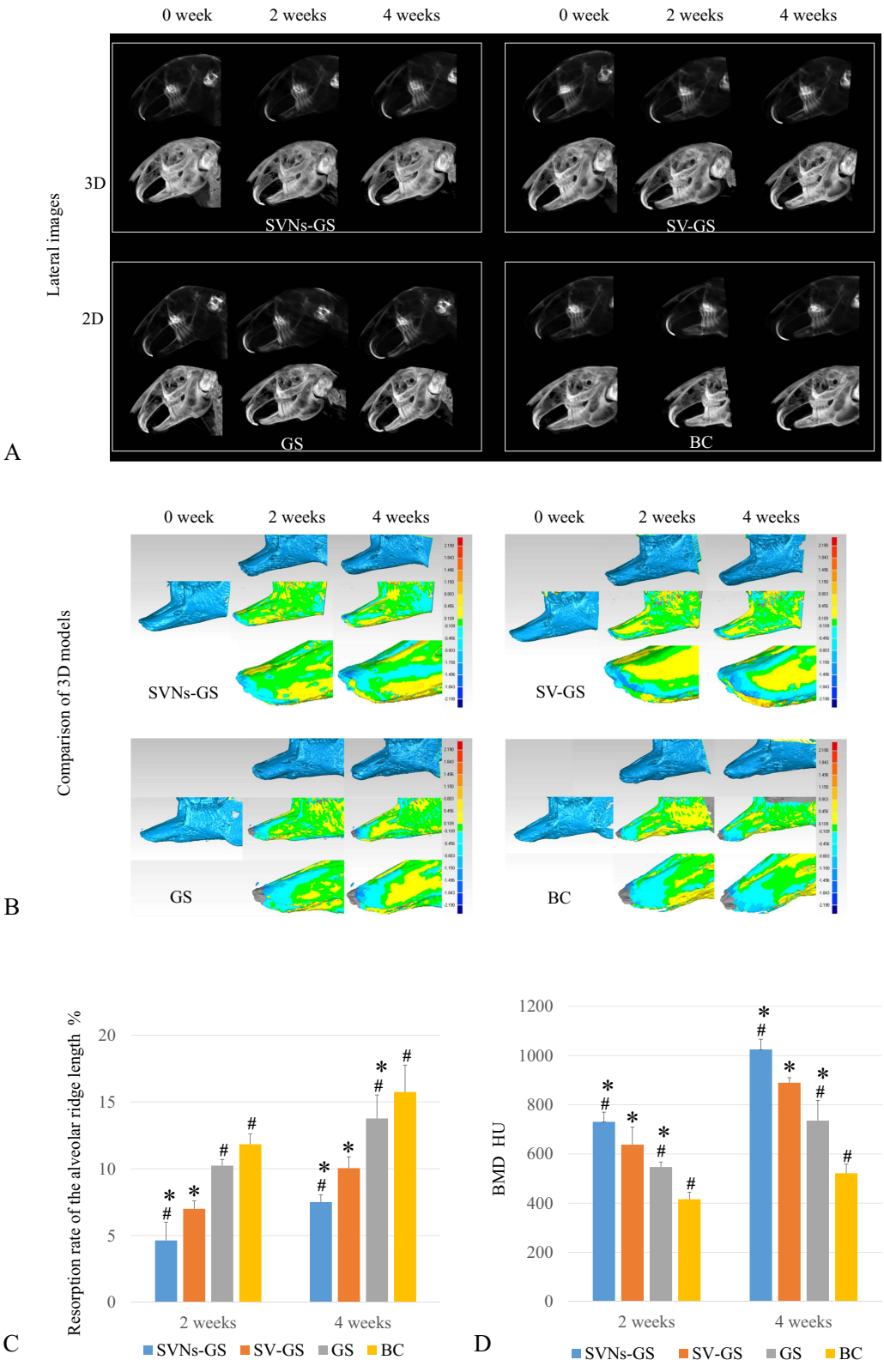

Figure 4 The results of CBCT analysis of the new bone formation in the extraction socket and alveolar ridge absorption at the tooth extraction sites. (**A**) The new bone formation and alveolar ridge absorption in each experimental group was performed by observing 2D and 3D lateral radiographs of the extraction socket. (**B**) Comparison of 3D images of alveolar ridge morphology at the extraction site. (**C**) The mean resorption rate of the alveolar ridge length at the extraction site in each experimental group at 2 weeks and 4 weeks (n=5). (**D**) The mean bone density of new bone in the extraction socket recorded in terms of CT values at 2 weeks and 4 weeks (n=5). The results are the mean values of five independent measurements (±SD) and were analysed by repeated-measures ANOVA. *$P<0.05$ vs BC; #$P<0.05$ vs SV-GS.

formation; in the SVNs-GS group, the formation of trabecular bone in the woven bone could be observed. Masson's trichrome staining showed that the new bone tissue in the BC group and the GS group was immature, with the collagen fibres appearing light blue; the new bone tissue in the SV-GS group and the SVNs-GS group was more mature than that in the BC and GS groups, with the collagen fibres staining blue or dark blue, and in particular, in the SVNs-GS group, the bone tissue in the trabecular area appeared red and blue, indicating ongoing or completed bone remodelling. (Figure 5A)

Under high magnification, HE staining showed that osteoblasts were densely arranged on the surface of the new bone tissue, while osteoclasts were occasionally observed in the BC and GS groups. The abundance of osteoclast was increased in the SV-GS group and SVNs-GS group (Figure 5B).

Discussion

ARP is an effective method for reducing bone resorption in the extraction socket area. A sufficient amount of bone mass remaining in the extraction socket area not only greatly shortens the time needed for oral implant restoration but also avoids additional trauma to the patient caused by bone grafting surgery. It has been confirmed that the addition of osteogenic growth factors can significantly improve the effect of synthetic materials on ARP.[22–24] However, exogenous osteogenic growth factors such as rhBMP-2 are not only expensive but also have the disadvantages of a short half-life and easy inactivation.

SV has been used in the clinical treatment of hypercholesterolemia since 1992. It is inexpensive, safe and reliable and has been included in the Model List of Essential Drugs by the World Health Organization, demonstrating that is an essential drug in the medical field. Previous studies have shown that SV can exert its osteogenic effect by regulating the expression of growth factors (such as BMP-2 and vascular endothelial growth factor) in osteoblasts.[25,26] However, SV has poor water solubility, a short half-life, and low affinity for bone, resulting in low bioavailability. Studies have shown that the efficacy of topical SV administration in promoting bone regeneration can be approximately 50-fold greater than that of oral administration.[27,28] Therefore, in this study, SV was loaded into a gelatin sponge and stuffed into the extraction socket to fully exploit the osteogenic effect of the drug.

Furthermore, some studies have shown that when administered topically, the osteogenic effect of SV is positively proportional to its dose within a certain range.[29] When the dose of SV is low, the time for SV to exert its drug effect is relatively short, and thus, it has a very limited osteogenic effect. Moreover, although increasing the topical dose of SV can prolong the duration of action of the drug, it may also cause local inflammation in the bone defect area and instead affect the normal process of bone regeneration.[30–32] In animal experiments, the optimal dose of simvastatin to stimulate maximal bone regeneration without inducing inflammation would be 0.1–0.5 mg.[33] In the rabbit calvarial defect bone regeneration model, it is suitable to add 0.5 mg of SV to each circular bone defect area with a diameter of 6–8 mm.[20,34–36] A suitable local dose of SV for the preservation of rabbit tooth extraction sites has not been clearly reported. Therefore, to ensure that SVNs can exert its effect as long as possible while avoiding causing inflammation in local tissues, and thus affecting the normal healing of the extraction socket, in the present experiment, we added 0.5 mg of SV and 5 mg SVNs (containing 0.5mg SV) to extraction socket. Histological sections showed no inflammation around the extraction socket, indicating that the dose selection of SVNs and SV was relatively reasonable.

In addition, on the basis of local application, increasing the dose of SV as much as possible and allowing its slow and sustained release are effective strategies for further enhancing the osteogenic effect of SV.[15] The sustained release of SV can be achieved by using nanodrug carriers to encapsulate SV and modify it to a nanoscale dose. Our previous studies showed that synthetic SVNs prolonged the release time of SV by more than 10-fold, significantly improved the efficacy of SV in promoting osteoblast differentiation and exhibited a stronger ability to promote bone regeneration in rabbit calvarial defect repair.[20] On this basis, the present study applied SVNs to the experiment of tooth extraction site preservation.

Imaging findings showed that at 2 and 4 weeks after tooth extraction, the gelatin sponge alone increased the new bone density in the extraction socket by 31.5% and 41.0%, respectively, compared with that in the BC group, promoting new bone formation in the extraction socket to some extent. When SV was used in combination with gelatin sponge, the rate of new bone formation in the extraction socket significantly increased. When SVNs were used in place of SV in

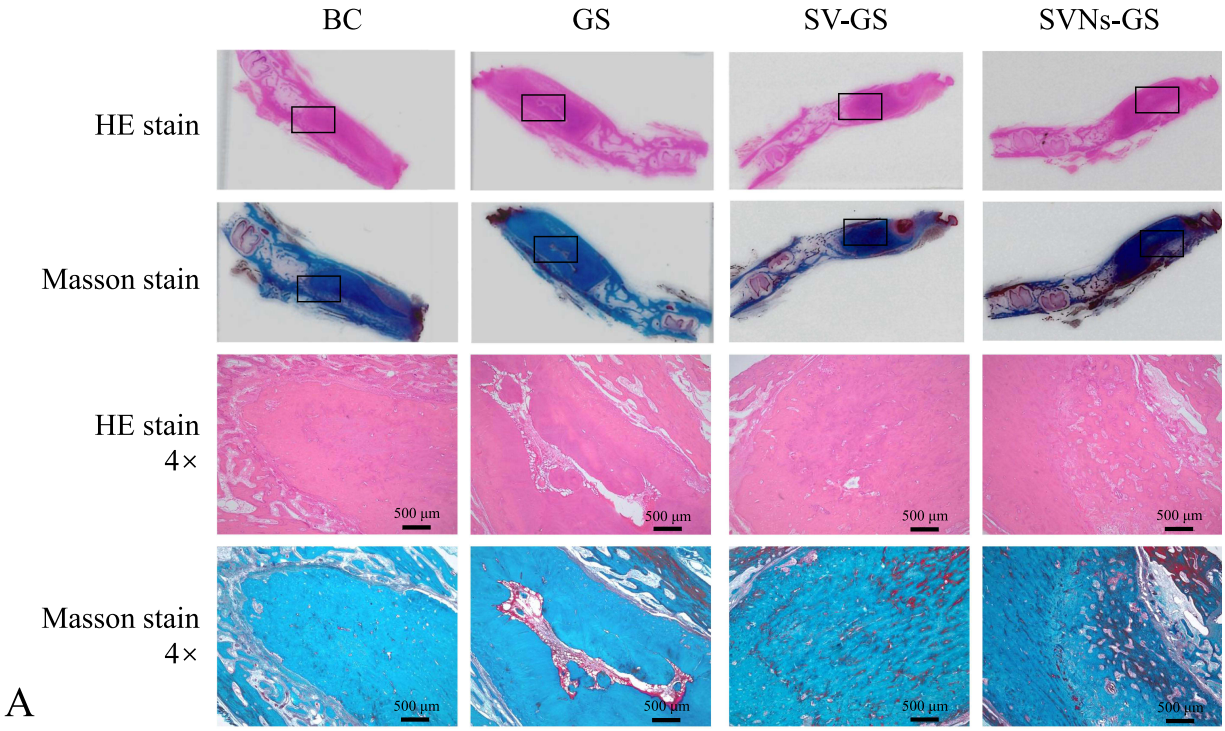

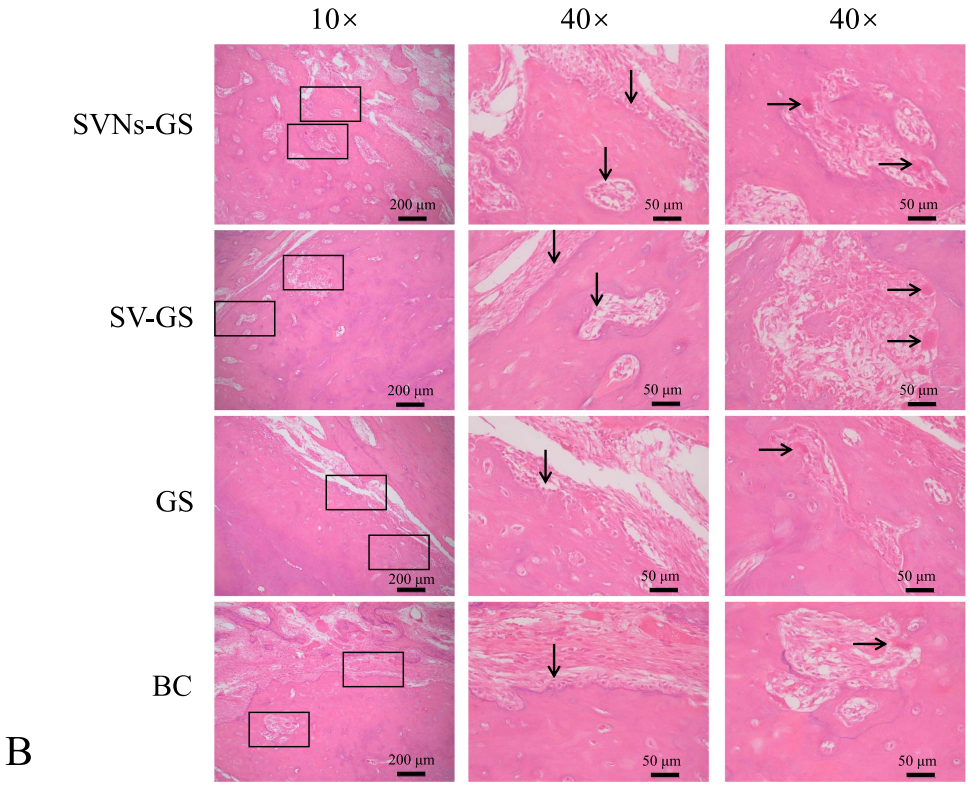

Figure 5 The results of histological analysis of the new bone formation in the extraction socket. (**A**) Histologic images of the new bone formation in the extraction socket at four weeks (HE stain and Masson stain, ×4). (**B**) Histologic images of the new bone formation in the extraction socket at four weeks (HE stain, ×10, ×40, ×40). The arrows "↓" indicate osteoblasts, The arrows "→" indicate osteoclasts.

combination with gelatin sponge, compared with that in the BC group, the new bone density in the extraction socket increased by 75.7% and 96.5%, respectively.

After tooth extraction, osteoblasts form the initial immature bone tissue. Thereafter, osteoclasts gradually increased in the new bone tissue. The osteogenesis of osteoblasts and the osteoclastogenesis of osteoclasts cooperate to remodel the new bone.[37] The morphology and structure of the new bone tissue are continuously adjusted, and the immature bone tissue gradually becomes strong and dense, and finally forms mature bone tissue. The histological results of this study showed that at 4 weeks, the maturity of new bone tissue in the extraction socket was low in the BC and GS groups, and the number of osteoclasts was small, indicating that bone remodelling occurred less frequently. In contrast, bone tissue maturity and active bone remodelling were greater in the SV-GS group and the SVNs-GS group. In particular, in the new bone tissue of the SVNs-GS group, a trabecular structure was observed. All of the above results show that SVNs significantly accelerated the process of bone healing in the extraction socket and significantly improved the efficacy of SV in promoting new bone formation.

The ability of the same material or drug to promote the healing of the extraction socket and reduce the resorption of the alveolar ridge varied. According to the calculated mean resorption rate of the alveolar ridge length at the extraction site at 2 and 4 weeks after tooth extraction, compared with the BC, the gelatin sponge promoted the formation of new bone in the extraction socket but had very limited effect on the preservation of the alveolar ridge length. The use of the gelatin sponge in combination with SV or SVNs significantly reduced the resorption of the alveolar ridge length after tooth extraction. In particular, the resorption rate of the alveolar ridge length was reduced in the SVNs group by 60.8% and 49.1% compared to that in the BC group at 2 and 4 weeks after tooth extraction, suggesting that SVNs significantly enhanced the effect of SV on ARP at the extraction site. The comparison of the 3D models of the alveolar ridge before and after tooth extraction found that, besides the length reduction, there was varying degrees of bone resorption on the surface of the alveolar ridge, which decreased the height and width of the alveolar ridge. The use of SVNs not only significantly reduced the resorption of the alveolar ridge at the extraction site but also played an important role in maintaining the size of the alveolar ridge.

This study has several limitations. First, the healing of the extraction socket generally lasts for 3 months, while this study focused on the investigation of the effect of SVNs in the early stage of tooth extraction site preservation. Second, the suitable local dosage of SV for preservation at the extraction site in rabbits is still unclear. Third, because the dose of SVNs applied topically is low, the sustained release effect of SVNS in vivo was not evaluated. Subsequent research should be conducted on the above three aspects to further optimize the local drug dose of SVNs and achieve longer sustained release of the drug and provide a more objective and accurate evaluation of the role of SVNs in the whole process of bone healing and ARP in the extraction socket.

Conclusion

In this study, SVNs were loaded on a gelatin sponge, which was then placed in the tooth extraction sockets of rabbits. The radiological and histological results showed that, in the early stage of extraction socket healing, SVNs could accelerate the formation of new bone in the extraction socket by increasing the number of osteoblasts, and accelerate the occurrence of bone remodeling by regulating the proportion of osteoblasts and osteoclasts, thereby effectively increasing the bone density in the extraction socket and significantly accelerating the healing of the extraction socket. Meanwhile, SVNs can effectively reduce the absorption of alveolar ridge length and volume at tooth extraction sites, showing promising application prospects in the preservation of tooth extraction sites.

Acknowledgment

This work was supported by grants from Shenzhen Basic Research Fund (6021210053K) and the Special projects in key areas of Guangdong Province (No.2022ZDZX2083).

Disclosure

The authors report no conflicts of interest in this work.

References

1. Irinakis T. Rationale for socket preservation after extraction of a single-rooted tooth when planning for future implant placement. *J Can Dent Assoc*. 2006;72(10):917–922.
2. Farmer M, Darby I. Ridge dimensional changes following single-tooth extraction in the aesthetic zone. *Clin Oral Implants Res*. 2014;25(2):272–277. doi:10.1111/clr.12108
3. Tan WL, Wong TL, Wong MC, et al. A systematic review of post-extractional alveolar hard and soft tissue dimensional changes in humans. *Clin Oral Implants Res*. 2012;23 Suppl 5(s5):1–21. doi:10.1111/j.1600-0501.2011.02375.x
4. Yuan J, Cui L, Zhang WJ, et al. Repair of canine mandibular bone defects with bone marrow stromal cells and porous beta-tricalcium phosphate. *Biomaterials*. 2007;28(6):1005–1013. doi:10.1016/j.biomaterials.2006.10.015
5. Darby I, Chen ST, Buser D. Ridge preservation techniques for implant therapy. *Int J Oral Maxillofac Implants*. 2009;24 Suppl:260–271.
6. Zhu W, Li C, Yao M, et al. Advances in osseointegration of biomimetic mineralized collagen and inorganic metal elements of natural bone for bone repair. *Regen Biomater*. 2023;10:rbad30. doi:10.1093/rb/rbad030
7. Wang YWY, Zhang HZH, Hu Y, et al. Bone repair biomaterials a perspective from immunomodulation. *Adv Funct Mater*. 2022;51(32):2208639.
8. Baykan E, Koc A, Eser EA, et al. Evaluation of a biomimetic poly(ε-caprolactone)/β-tricalcium phosphate multispiral scaffold for bone tissue engineering:in vitro and in vivo studies. *Biointerphases*. 2014;9(2):29011. doi:10.1116/1.4870781
9. Ohgushi H, Caplan AI. Stem cell technology and bioceramics: from cell to gene engineering. *J Biomed Mater Res*. 1999;48(6):913–927. doi:10.1002/(SICI)1097-4636(1999)48:6<913::AID-JBM22>3.0.CO;2-0
10. Jones JR, Ehrenfried LM, Hench LL. Optimising bioactive glass scaffolds for bone tissue engineering. *Biomaterials*. 2006;27(7):964–973. doi:10.1016/j.biomaterials.2005.07.017
11. Zeng JH, Qiu P, Xiong L, et al. Bone repair scaffold coated with bone morphogenetic protein-2 for bone regeneration in murine calvarial defect model: systematic review and quality evaluation. *Int J Artif Organs*. 2019;42(7):325–337. doi:10.1177/0391398819834944
12. Han JJ, Chang AR, Ahn J, et al. Efficacy and safety of rhBMP/beta-TCP in alveolar ridge preservation: a multicenter, randomized, open-label, comparative, investigator-blinded clinical trial. *Maxillofac Plast Reconstr Surg*. 2021;43(1):42. doi:10.1186/s40902-021-00328-0
13. Moslemi N, Khoshkam V, Rafiei SC, et al. Outcomes of alveolar ridge preservation with recombinant human bone morphogenetic protein-2: a systematic review. *Implant Dent*. 2018;27(3):351–362. doi:10.1097/ID.0000000000000722
14. Mundy G, Garrett R, Harris S, et al. Stimulation of bone formation in vitro and in rodents by statins. *Science*. 1999;286(5446):1946–1949. doi:10.1126/science.286.5446.1946
15. Diniz JA, Dourado A, Barbirato D, et al. Effect of simvastatin topical use on alveolar bone after tooth extraction: a scoping review. *Clin Oral Investig*. 2024;28(1):86. doi:10.1007/s00784-023-05482-5
16. Xu L, Wang C, Shen WW, et al. Effects of simvastatin nano-liposomes on osteogenic differentiation of bone marrow stromal cells. *Beijing Da Xue Xue Bao Yi Xue Ban*. 2014;46(6):883–888.
17. Liu X, Li X, Zhou L, et al. Effects of simvastatin-loaded polymeric micelles on human osteoblast-like MG-63 cells. *Colloids Surf B Biointerfaces*. 2013;102:420–427. doi:10.1016/j.colsurfb.2012.06.037
18. Naito Y, Terukina T, Galli S, et al. The effect of simvastatin-loaded polymeric microspheres in a critical size bone defect in the rabbit calvaria. *Int J Pharm*. 2014;461(1–2):157–162. doi:10.1016/j.ijpharm.2013.11.046
19. Wu Z, Liu C, Zang G, et al. The effect of simvastatin on remodelling of the alveolar bone following tooth extraction. *Int J Oral Maxillofac Surg*. 2008;37(2):170–176. doi:10.1016/j.ijom.2007.06.018
20. Feng X, Yue X, Niu M. Simvastatin-loaded nanomicelles enhance the osteogenic effect of simvastatin. *J Nanomater*. 2020;2020:1–14. doi:10.1155/2020/1072765
21. Niu M, Feng X, Zhou L. The role of the ERK1/2 pathway in simvastatin-loaded nanomicelles and simvastatin in regulating the osteogenic effect in MG63 cells. *Int J Nanomed*. 2018;13:8165–8178. doi:10.2147/IJN.S182998
22. Jafer MA, Salem RM, Hakami FB, et al. Techniques for extraction socket regeneration for alveolar ridge preservation. *J Contemp Dent Pract*. 2022;23(2):245–250. doi:10.5005/jp-journals-10024-3247
23. Ucer C, Khan RS. Extraction socket augmentation with autologous platelet-rich fibrin (PRF): the rationale for socket augmentation. *Dent J*. 2023;11(8)196.
24. Samandari MH, Haghighat A, Torabinia N, et al. Socket preservation using freeze-dried bone allograft with and without plasma rich in growth factors in dogs. *Dent Res J*. 2016;13(5):432–439. doi:10.4103/1735-3327.192290
25. Wang Z, Li Y, Zhou F, et al. Effects of statins on bone mineral density and fracture risk. *Medicine*. 2016;95(22):1–8.
26. Grifths SL, Cartmell SH. Use of statins for enhancing bone-tissue-engineered grafts. *Eur J Plast Surg*. 2012;35:151–157. doi:10.1007/s00238-007-0190-2
27. Gutierrez GE, Lalka D, Garrett IR, et al. Transdermal application of lovastatin to rats causes profound increases in bone formation and plasma concentrations. *Osteoporos Int*. 2006;17(7):1033–1042. doi:10.1007/s00198-006-0079-0
28. Diniz JA, Barbirato D, Do NE, et al. Tomographic evaluation of the effect of simvastatin topical use on alveolar bone microarchitecture, pain and swelling after mandibular third molar extraction: a randomized controlled trial. *Clin Oral Investig*. 2022;26(4):3533–3545. doi:10.1007/s00784-021-04322-8
29. Kheirallah M, Almeshaly H. Simvastatin, dosage and delivery system for supporting bone regeneration, an update review. *J Oral Maxillofac Surg Med Pathol*. 2016;28(3):205–209. doi:10.1016/j.ajoms.2015.10.005
30. Nyan M, Miyahara T, Noritake K, et al. Molecular and tissue responses in the healing of rat calvarial defects after local application of simvastatin combined with alpha tricalcium phosphate. *J Biomed Mater Res B Appl Biomater*. 2010;93(1):65–73. doi:10.1002/jbm.b.31559
31. Thylin MR, McConnell JC, Schmid MJ, et al. Effects of simvastatin gels on murine calvarial bone. *J Periodontol*. 2002;73(10):1141–1148. doi:10.1902/jop.2002.73.10.1141
32. Stein D, Lee Y, Schmid MJ, et al. Local simvastatin effects on mandibular bone growth and inflammation. *J Periodontol*. 2005;76(11):1861–1870. doi:10.1902/jop.2005.76.11.1861
33. Chen S, Yang JY, Zhang SY, et al. Effects of simvastatin gel on bone regeneration in alveolar defects in miniature pigs. *Chin Med J*. 2011;124(23):3953–3958.

34. Lee Y, Schmid MJ, Marx DB, et al. The effect of local simvastatin delivery strategies on mandibular bone formation in vivo. *Biomaterials*. 2008;29 (12):1940–1949. doi:10.1016/j.biomaterials.2007.12.045
35. Yue X, Niu M, Zhang T, et al. In vivo evaluation of a simvastatin-loaded nanostructured lipid carrier for bone tissue regeneration. *Nanotechnology*. 2016;27(11):115708. doi:10.1088/0957-4484/27/11/115708
36. Wong RWK, Rabie ABM. Statin collagen grafts used to repair defects in the parietal bone of rabbits. *Br J Oral Maxillofac Surg*. 2003;41 (4):244–248. doi:10.1016/S0266-4356(03)00081-0
37. Kim JM, Lin C, Stavre Z, et al. Osteoblast-osteoclast communication and bone homeostasis. *Cells*. 2020;9(9):2073. doi:10.3390/cells9092073

International Journal of Nanomedicine Dovepress

Publish your work in this journal

The International Journal of Nanomedicine is an international, peer-reviewed journal focusing on the application of nanotechnology in diagnostics, therapeutics, and drug delivery systems throughout the biomedical field. This journal is indexed on PubMed Central, MedLine, CAS, SciSearch®, Current Contents®/Clinical Medicine, Journal Citation Reports/Science Edition, EMBase, Scopus and the Elsevier Bibliographic databases. The manuscript management system is completely online and includes a very quick and fair peer-review system, which is all easy to use. Visit http://www.dovepress.com/testimonials.php to read real quotes from published authors.

Submit your manuscript here: https://www.dovepress.com/international-journal-of-nanomedicine-journal